Journal of Membrane Science 493 (2015) 807–819

Contents lists available at ScienceDirect

Journal of Membrane Science

journal homepage: www.elsevier.com/locate/memsci

# Layer-by-layer surface modification of polyethersulfone membranes using polyelectrolytes and AgCl/$TiO_2$ xerogels

Papatya Kaner [a,1], Daniel J. Johnson [b], Erol Seker [a], Nidal Hilal [b], Sacide Alsoy Altinkaya [a,*]

[a] Department of Chemical Engineering, Izmir Institute of Technology, Gulbahce Campus, 35430 Urla, Izmir, Turkey
[b] Centre for Water Advanced Technologies and Environmental Research (CWATER), College of Engineering, Swansea University, Singleton Park, Swansea SA2 8PP, UK

ARTICLE INFO

*Article history:*
Received 12 January 2015
Received in revised form
18 May 2015
Accepted 23 May 2015
Available online 4 June 2015

*Keywords:*
Layer by layer assembly
Ultrafiltration membrane
Silver xerogel
Antifouling
Water treatment

ABSTRACT

In this study, the layer-by-layer (LbL) assembly method was employed to modify a commercial polyethersulfone (PES) membrane by successive adsorption of chitosan and alginate as cationic and anionic polyelectrolytes. To enhance anti-biofouling property, pure, PEG mixed and PEGylated AgCl/$TiO_2$ xerogels were incorporated solely in the top layer of the LbL-modified membranes. Organic and biological foulings were addressed separately using alginate and *Escherichia coli* bacteria suspensions as the organic and biological model foulants, respectively. LbL-modifying the commercial PES membrane successively with chitosan and alginate polyelectrolyte multilayers prevented organic fouling extensively. In addition, we found that AgCl/$TiO_2$-incorporated membranes show higher water permeability and improved resistance to biological fouling as compared to the PES membrane. Silver amounts in consecutively collected permeate samples were quantified by ICP-MS analysis to assess the stability of AgCl/$TiO_2$-incorporated layers. Silver loss per filtration cycle followed an increasing trend initially, up to a filtration volume totaling 3000 L/$m^2$, leading to 4.2% reduction in the immobilized silver amount. After that, silver loss per filtration cycle stabilized at ~7.44 μg/L, which extrapolates to ~265 days time-span for the remaining silver to be released at a filtration rate of ~1000 L/$m^2$ h. Antibacterial activity tests showed that AgCl/$TiO_2$-incorporated layers do not permit bacterial growth on the membrane surface.
© 2015 Elsevier B.V. All rights reserved.

## 1. Introduction

Organic and biological foulings still comprise significant obstacles to the wider use of membranes in water treatment. Membrane fouling may take place due to partial pore size reduction as a consequence of foulants such as humic acids, colloids, bacteria etc. in water, adsorbing on the inner pore walls, pore blockage and cake or gel formation on the surface, causing high operation costs, high energy input, the need for frequent cleaning and reduced membrane life-span [1]. Several methods focus on employing surface modification procedures that tune the surface charge or increase hydrophilicity to prevent adsorption of foulants onto the surface [2].

Grafting and layer-by-layer (LbL) polyelectrolyte coating have been proposed as two promising surface modification methods, especially for membranes used in desalination of brackish and seawater, reclamation of wastewater, membrane bioreactors (MBR), and other industrial separations [3]. Although surface grafting enhances fouling resistance, it results in permanent change of membrane chemistry and properties [4]. In addition, grafting may cause increased manufacturing costs because of process complications, time loss, and substantial consumption of organic solvents and monomers [5]. Compared to grafting, LbL coating of water-soluble polymers from solution by the successive adsorption of polyanions and polycations onto the charged surface of a thick, porous base membrane appears to be more advantageous for membrane modification [4,6] because polyelectrolyte multilayer (PEM) deposition is straightforward to conduct and the base membrane itself remains intact while the adsorbed molecules alter the surface only.

Ba et al. [6] observed the improved fouling resistance for P84 copolyimide when a positively charged polyethylenimine followed by a layer of water-soluble polymer was adsorbed onto the membrane surface. Similarly, Wang et al. [7] applied layer-by-layer deposition of sulfonated poly(ether ether ketone) (sPEEK) and branched polyethyleneimine (PEI) onto polyacrylonitrile membranes and obtained improved antifouling property in comparison with the commercial membrane NTR 7450. Ba and Economy [3] developed a nearly neutrally charged nanofiltration membrane by adsorbing a negatively charged sulfonated poly (ether ether ketone) (SPEEK) onto the surface of a positively

* Corresponding author. Tel.: +90 2327506658; fax: +90 2327506645.
*E-mail address:* sacidealsoy@iyte.edu.tr (S.A. Altinkaya).
[1] Present address: Department of Chemical and Biological Engineering, Tufts University, Medford, MA 02155, US.

http://dx.doi.org/10.1016/j.memsci.2015.05.048
0376-7388/© 2015 Elsevier B.V. All rights reserved.

charged NF membrane. It was found that the surface charge had a significant influence on multivalent ion rejection and fouling resistance. In addition, Lajimi et al. [8] showed decreased fouling for LbL-modified cellulose acetate (CA) membranes by sequential deposition of chitosan/alginate polyelectrolyte pairs.

Although the above studies have shown that PEMs enhance surface properties against organic fouling, biological fouling prevention with PEMs remains fairly unexplored. To prevent bacterial growth and biofilm formation, antibacterial materials, such as silver, chitosan, quaternary ammonium groups, photocatalytic $TiO_2$, and ethylene glycol oligomer, have been incorporated into or onto membrane surfaces following different routes [9–12]. Among these, silver based materials were frequently used due to their high antimicrobial activity. For example, Zodrow et al. [10] impregnated silver nanoparticles into polysulfone matrix to improve biofouling resistance. Silver nanoparticles have commonly been attached covalently to the membrane surface to obtain high concentration of nanoparticles and therefore, antibacterial activity, at the membrane surface where the contact with the bacteria takes places [13]. Diagne et al. [14] modified the surface of commercially available polyethersulfone (PES) membranes using the polyelectrolyte multilayer modification method with poly(styrenesulfonate) (PSS), poly(diallyldimethylammonium chloride) (PDADMAC), and silver nanoparticles integrated onto the surface as stable, thin films. Filtration and cleaning studies showed that modification could significantly reduce organic and biological foulings. Despite the fact that silver nanoparticles have proven effective in preventing biofilm formation, uncontrolled silver release is still a major concern in silver-incorporated membranes because the antibacterial life span of a membrane is dependent on its silver retention. Only a few studies propose alternative approaches to slow the release of $Ag^+$ ions [13,15]. In general, the challenge in preparing membranes with silver based materials is to achieve the controlled release of silver and also, to specifically place silver materials on the top layer of the membrane. These challenges could be addressed by immobilizing the sol–gel made $AgCl/TiO_2$ xerogels on the membrane surface using the LbL assembly technique, which is promising in providing control over the silver release due to the low dissolution of AgCl. To the best of our knowledge, there are no studies on the modification of commercial polyethersulfone (PES) membranes with $AgCl/TiO_2$ xerogels incorporated into PEMs.

In this manuscript, we present the organic and biological fouling resistances performance of LbL-modified PES membrane with chitosan (CHI) and alginate (ALG) PEMs alone or PEMs incorporated with sol–gel made $AgCl/TiO_2$ xerogels. ALG is used as the model organic foulant to study organic fouling resistance and *Escherichia coli* suspension is used as the model biological foulant to study biological fouling resistance. In addition, antibacterial activities of the unmodified PES membrane, $AgCl/TiO_2$-free and $AgCl/TiO_2$-incorporated LbL-modified membranes are tested. The long-term stability and silver release rate from $AgCl/TiO_2$-incorporated membranes were evaluated by analyzing the permeate samples collected from consecutive filtration experiments.

## 2. Experimental

### 2.1. Materials

Low molecular weight chitosan (CHI) with molecular weight range of 40–90 kDa, alginic acid sodium salt from brown algae (ALG), and polyethylene glycol (PEG) with molecular weight 6000 Da ($M_n$=6000 Da) were purchased from Sigma-Aldrich Co., USA and used as received. Sodium hydroxide in pellets, hydrochloric acid 37%, sodium chloride, 2-propanol and acetic acid were also purchased from Sigma-Aldrich Co., USA and used without further purification.

In the synthesis of silver chloride containing titania ($AgCl/TiO_2$) xerogels, silver nitrate (99% purity, from Sigma-Aldrich Co., USA) was used as a silver precursor. Tetrabutyl-orthotitanate (TBOT) (99% purity, from Sigma-Aldrich Co., USA), nitric acid (65% purity, from Sigma-Aldrich Co., USA) and ethanol (99% purity, from Sigma-Aldrich Co., USA) were used without further purification. Reagent-grade deionized water (DI) was used in preparation of aqueous solutions (Arium 61316 water purification system, Sartorius).

Mueller-Hinton broth (OXOID Ltd., England), Mueller-Hinton agar (Sigma-Aldrich Co., USA) and bacteriological peptone (OXOID Ltd., England) were used to carry out the antibacterial activity tests. *E. coli* (ATCC 25922) was chosen as the test microorganism.

### 2.2. Polyelectrolyte solutions

#### 2.2.1. Alginate and chitosan solutions

Polyelectrolytes, CHI and ALG powder, were dissolved in aqueous medium at two concentrations, 0.1 and 1 g/L. CHI solution was prepared by dissolving a specified amount of CHI powder in 1% (v/v) acetic acid solution and ALG solution was obtained by dissolving in pure water. Both polyelectrolyte solutions were prepared by dissolving overnight under stirring condition to ensure that the powder is uniformly distributed in solution. Lastly, the pH of the CHI and ALG solutions were adjusted by addition of NaOH and HCl to 5 and 7, respectively.

#### 2.2.2. $AgCl/TiO_2$-incorporated chitosan solutions

Xerogels are made by sol–gel chemistry and drying, where the materials are produced from simple metal or metalloid precursors. A sol–gel process combines the particles obtained in a stabilized colloidal suspension, termed a sol, into a macroscopic molecule expanding in three dimensions in liquid, termed a gel. When the solvent is removed from the gel at a certain temperature under the atmospheric pressure, the solid material, called xerogel, is obtained. The character and morphology of xerogels can be adjusted for various applications by changing the starting reagents, catalyst, reaction environment and reaction environment of the sol–gel process [16].

In this study, silver chloride containing titania ($AgCl/TiO_2$) xerogels with 29 wt% AgCl content were incorporated into the outmost layer of CHI polyelectrolyte. $AgCl/TiO_2$ xerogels were synthesized following successively the sol–gel procedure steps (a) HCl sol–gel route II, and (b) additional HCl treatment sol–gel route III, as described by Tuncer and Seker [17]. In fact, these (a) and (b) approaches resulted in only $AgCl/TiO_2$ xerogels while other approaches used in Ref. [17] yielded $Ag/TiO_2$ xerogels. We confirmed these using XRD analysis of the xerogels synthesized in this study as seen in XRD patterns given in the Supplementary data Fig. A1. Silver nitrate was used as a silver precursor. Pure $AgCl/TiO_2$ at different concentrations, polyethylene glycol-mixed $AgCl/TiO_2$ or PEGylated $AgCl/TiO_2$ was incorporated in the outmost layer CHI polyelectrolyte solution. PEGylation involves the successive steps; washing polyethylene glycol (PEG) pellets with deionized water, mixing PEG solution with $AgCl/TiO_2$ xerogels, centrifuging the resulting solution and disposal of the supernatant to use the precipitate in preparation of polyelectrolyte solution. Dispersion of pure, PEG-mixed or PEGylated $AgCl/TiO_2$ into the CHI solution was accomplished by mixing the solution with a Homogenizer (IKA, T-18 TURRAX) and then sonicating with an Ultrasonic Cleaner (Elmasonic). The $AgCl/TiO_2$-incorporated CHI solutions include: (1) 0.1 g/L CHI and, 0.5, 1, 2.5 or 5 g/L $AgCl/TiO_2$, (2) 0.1 g/L CHI, 0.5 g/L $AgCl/TiO_2$ and 0.05 g/L PEG, and (3) 0.1 g/L CHI and PEGylated 0.5 g/L $AgCl/TiO_2$.

### 2.3. Preparation of LbL-modified PES membranes

The characteristics of commercial base polyethersulfone (PES) ultrafiltration membranes, provided by Microdyn Nadir of Germany under the code NADIR® PM UP150, are summarized in Table 1. Prior to use, PES membranes were subjected to a three-step pretreatment process, they were first kept in deionized water for 1 h, and then in 25% (v/v) 2-propanol solution for 1 h, followed by overnight storage in deionized water.

In LbL modification, each layer serves as a surface primer for the next oppositely charged layer. PES membranes are negatively charged, therefore the first layer adsorbed is the polycation CHI. A negatively charged ALG solution is subsequently added, which adheres to the CHI layer via electrostatic interactions and van der Waals forces. In this work, clean PES membrane coupon is placed in a holder with the active surface facing upward and the surface is exposed to the polyelectrolyte solution for a certain period of time at room temperature. Then, the membrane is washed with deionized water for 30 min to remove any loosely bound polyelectrolyte before immersion into the next polyelectrolyte solution. The cycle is repeated until the desired number of layers is achieved. Fig. A2 (Supplementary data) depicts the process of CHI polycation and ALG polyanion deposition on a negatively charged PES membrane.

LbL-modified PES membranes have been studied with respect to alterations in the CHI/ALG polyelectrolyte concentrations, adsorption time, number of bilayers, ionic strength and pH of the polyelectrolyte solution. Polyelectrolyte concentration was varied to 0.1 g/L and 1 g/L at adsorption times of 30 and 60 min. Number of modification layers employed were single layer $(CHI)_1$, 1.5 bilayers $(CHI/ALG)_1CHI$, 2.5 bilayers $(CHI/ALG)_2CHI$ and 3.5 bilayers $(CHI/ALG)_3CHI$ using 0.1 g/L or 1 g/L polyelectrolytes at 30 min adsorption time. In the experiments that address the influence of ionic strength of the PEMs, 1 g/L polyelectrolyte solutions were prepared with 0.1 M NaCl to make 1.5, 2.5 and 3.5 bilayer membranes. For exploiting the effects of outmost layer CHI solution pH, 1.5 bilayer membranes were produced by using 0.1 g/L CHI solution with the pH adjusted to 5 or 6. All these modified membranes were then tested by filtration and antifouling experiments. The better performing membranes were then used for physical characterization and antibacterial activity analysis.

$AgCl/TiO_2$ xerogels were added into the outmost layer of $(CHI)_1$ and $(CHI/ALG)_1CHI$ membranes to impart anti-biofouling and antibacterial properties to these membranes. Pure $AgCl/TiO_2$ at different concentrations, polyethylene glycol-mixed $AgCl/TiO_2$ and PEGylated $AgCl/TiO_2$ were used in the modifications. In $(CHI)_1$ membrane, the polyelectrolyte solution was prepared to result in 0.1 g/L CHI and, 0.5, 1 or 5 g/L $AgCl/TiO_2$ xerogels. The outmost layer polyelectrolyte of $(CHI/ALG)_1CHI$ membranes included: (1) 0.1 g/L CHI and, 0.5, 1 or 2.5 g/L $AgCl/TiO_2$, (2) 0.1 g/L CHI, 0.5 g/L $AgCl/TiO_2$ and 0.05 g/L PEG, and (3) 0.1 g/L CHI and PEGylated 0.5 g/L $AgCl/TiO_2$. The $AgCl/TiO_2$-incorporated membranes were used in filtration, anti-biofouling, physical characterization and antibacterial activity tests.

**Table 1**
Characteristics of the commercial PES membrane.

| Membrane material | Abbreviation | Unmodified membr. permeability L/(m².h.bar) | Contact angle (deg) |
|---|---|---|---|
| Polyethersulfone | PES | 921±41 | 55.3±4.7 |

### 2.4. Physical characterization

#### 2.4.1. Membrane surface morphology by scanning electron microscopy (SEM)

SEM imaging was used to assess the morphology of unmodified and LbL-modified membranes. Both the membrane upper surfaces and cross-sections through the membrane were examined, using an Ultra-High Resolution FE-SEM (Hitachi). Cross-sections were obtained by first immersing the membrane in liquid nitrogen and then cutting from the reverse side using a fresh razor blade. All samples were sputter-coated with an approximately 15 nm thick layer of gold prior to imaging. The EDX mapping was conducted with 500 × magnification.

#### 2.4.2. Membrane surface roughness by atomic force microscopy (AFM)

AFM measurements were carried out using a Multimode AFM with a Nanoscope IIIa controller (Bruker). All measurements were performed using tapping mode in high purity water. Samples were kept wet throughout sample preparation and during measurements to prevent structural changes, which may otherwise occur due to drying out of the membranes. Samples were immobilized onto metal sample mounting disks using an adhesive able to cure in aqueous solution. Roughness values were obtained directly from scanned images using the instrument software.

#### 2.4.3. Membrane surface charge by staining

To measure the surface charge of the membranes, they were stained with the cationic dye Toluidine Blue O and anionic dye Congo red using the protocol suggested by Tiraferri and Elimelech [18]. Dye solutions with concentrations of 30 ppm were prepared and the pH was adjusted to 7. Membranes with 4 $cm^2$ surface area were attached to the glass surface, 2 ml of dye solution was dropped on the active surface of the membranes and they were incubated for 30 min at room conditions. Then, the membranes were washed with 20 ml distilled water for 30 min, dried at room conditions and the amount of charged groups on the membranes stained with toluidine blue O and congo red was determined spectrophotometrically (Aventes Avemouse62) by measuring the intensity of each color resulting from adsorption of dyes on the membranes. Each intensity value was reported as an average of 20 measurements.

### 2.5. Filtration tests

Filtration and fouling tests were carried out using a dead-end cell filtration system (Model 8050, Milipore Corp., Bedford, MA) with a total internal volume of 50 ml and active surface area of 13.4 $cm^2$. In the filtration tests, a circular flat sheet membrane was placed into the permeation cell and its position was fixed with an O-ring. Membrane compaction was conducted at 100 kPa prior to any filtration test to ensure steady state conditions. Then, deionized water was filtered through the membrane at 70 kPa, where the permeate was collected in a vessel mounted on a balance. The volumetric flux of water was calculated from the slope of the permeate volume vs. time graph and converted to hydraulic permeability.

### 2.6. Organic and biological fouling tests

We used two routes to address organic and biological fouling resistances separately. Organic fouling resistance was tested by monitoring the water permeability decline after filtering 0.1 g/L

ALG solution at pH 7, a procedure applied to mimic the natural organic fouling of water treatment membranes. In each organic fouling test, membrane compaction was conducted at 100 kPa to reach steady state first, and then ALG solution was filtered for 4 h at 70 kPa. The reduction in water permeability caused by organic fouling was calculated from the difference between water permeability after fouling ($WF_f$) and before fouling ($WF_i$):

$$\%\ \text{Decline in permeability} = \left(\frac{WF_i - WF_f}{WF_i}\right) \times 100$$

For testing biological fouling resistance of the LbL-membranes, *E. coli* suspension was employed as the model biological foulant. Target *E. coli* was cultured to a midlog phase on Mueller-Hinton agar at 37 °C. The cells were harvested by picking off bacteria colonies with a swap from the Mueller-Hinton agar plate, added into 0.1% (w) peptone water to sustain a Mc Farland value of 0.5, which corresponds to $10^8$ Colony Forming Units per milliliter (CFU/ml), and then resuspended in a solution with the cell concentration to result in approximately $10^7$ CFU/mL. 100 mL of this mixture was filtered through the membranes to inflict biological fouling on the membrane surface. Reduction in water flux due to *E. coli* suspension filtration was used to determine biological fouling tendency.

### 2.7. Stability

The stability of the $AgCl/TiO_2$-free surface layers during wash with NaCl solution was characterized by comparing the membrane water fluxes at 70 kPa obtained immediately after LbL modification, and after storage in 1 M NaCl solution for 7 and 14 days, subsequently.

The silver leaching of $AgCl/TiO_2$-incorporated layers was assessed by following the silver content in the permeate samples collected during deionized water filtration through the membranes using a dead-end cell filtration system (Model 8200, Millipore Corp., Bedford, MA) with a total internal volume of 200 ml and active surface area of 28.7 $cm^2$. The filtration was conducted at 70 kPa, and the permeate samples were acquired in 13 ml aliquots. The silver concentration in the permeate samples was quantified using a 7500ce Series inductively coupled plasma quadruple mass spectrometer (ICP-MS) (Tokyo, Japan) without further dilution.

### 2.8. Antibacterial tests

*E. coli* was used as a model microorganism to evaluate the antibacterial activity of the membrane surfaces. Muller-Hinton broth and Mueller-Hinton agar were used as the growth media. The *E. coli* was cultured to a midlog phase on Mueller-Hinton agar at 37 °C. Following incubation, the initial *E. coli* concentration was adjusted by picking off bacteria colonies with a swap from the Mueller-Hinton agar plate and mixing with 0.1% (w) peptone water, till reached a Mc Farland value of 0.5, which corresponds to approximately $10^8$ CFU/ml. 100 μl of this *E. coli* solution was then added into 10 ml Mueller-Hinton broth in sterilized tubes to obtain a bacterial concentration of $\sim 10^6$ CFU/ml. Then, *E. coli* solution was serially diluted using Mueller-Hinton broth to 100 CFU/ml from the $10^6$ CFU/ml stock. Next 0.6 ml of the diluted solution, which corresponds to 60 CFU, was spread onto the membranes (membrane area: $5 \times 5$ $cm^2$). Prior to 24 h incubation at 37 °C on Mueller-Hinton agar plates, membranes were pre-incubated for 2 h to ensure complete adsorption of bacteria solution on the membrane surface. Following 24 h incubation, the number of bacteria present on the membrane surface was compared to the initial 60 CFU. LbL membranes with $AgCl/TiO_2$-free and $AgCl/TiO_2$-incorporated surfaces with different xerogel concentrations were tested against *E. coli*. As a control, the base PES membrane was also subjected to antibacterial activity test. Three replicates of each batch were prepared for the tests to provide statistical confidence. All the materials were sterilized at standard conditions, i.e. 120 °C, 15 psi and for 30 min before use.

## 3. Results and discussion

### 3.1. Physical characterization of the LbL-modified membranes

#### 3.1.1. Membrane surface morphology by scanning electron microscopy (SEM) and atomic force microscopy (AFM)

Table 2 lists the modified membranes studied in this section by SEM and AFM measurements.

SEM images at 5000× (Supporting data, Fig. A3) for all samples containing $AgCl/TiO_2$ xerogels show that the surface is covered in relatively large aggregates of xerogels. There appears to be little or no correlation between the concentration of xerogels used, the surface preparation or the quantity and size of the xerogel aggregates on the surface. Selected higher magnification SEM images (50,000×, Fig. 1 left column) show the finer structure of the membrane. Whilst the overall morphologies of the membrane surfaces are similar, showing the same basic morphology, from the AFM images (Fig. 1 right column) and the corresponding root mean square (RMS, Fig. 2) roughness values, it can be seen that the single layer membranes not subject to $AgCl/TiO_2$ xerogel surface treatments are generally lower in roughness than their $AgCl/TiO_2$-incorporated counterparts. Due to the small scan sizes used ($1 \times 1$ $\mu m^2$), this change in roughness cannot be related to the presence of large particulate agglomerations seen only in the low magnification SEM images, and is likely a consequence of the membrane morphology, showing a significant alteration to the surface structure due to the presence of the xerogels. As the height resolution of an AFM instrument is typically much less than 1 nm, and often sub-angstrom, the AFM is capable of picking up surface features which may affect the roughness that are below the resolution limits of the SEM to detect. $AgCl/TiO_2$-free and $AgCl/TiO_2$-incorporated 1.5 bilayer membranes are very similar in

**Table 2**
Single layer and 1.5 bilayer LbL-modified membranes analyzed by SEM and AFM.

| LbL layers | Polyelectr. conc. (g/L) | Modification agent | Abbreviation |
|---|---|---|---|
| CHI | 0.1 | - | 0.1-$(CHI)_1$ |
| CHI | 0.1 | 0.5 g/L $AgCl/TiO_2$ | 0.1-$(CHI)_1$-0.5Ag |
| CHI | 0.1 | 1 g/L $AgCl/TiO_2$ | 0.1-$(CHI)_1$-1Ag |
| CHI/ALG/CHI | 0.1 | - | 0.1-$(CHI/ALG)_1CHI$ |
| CHI/ALG/CHI | 1 | - | 1-$(CHI/ALG)_1CHI$ |
| CHI/ALG/CHI | 0.1 | 0.5 g/L $AgCl/TiO_2$ | 0.1-$(CHI/ALG)_1CHI$-0.5Ag |
| CHI/ALG/CHI | 0.1 | 1 g/L $AgCl/TiO_2$ | 0.1-$(CHI/ALG)_1CHI$-1Ag |
| CHI/ALG/CHI | 0.1 | 0.5 g/L $AgCl/TiO_2$+0.05 g/L PEG | 0.1-$(CHI/ALG)_1CHI$-0.5Ag-0.05PEG |
| CHI/ALG/CHI | 0.1 | 0.5 g/L PEGylated $AgCl/TiO_2$ | 0.1-$(CHI/ALG)_1CHI$-PEGylated 0.5Ag |

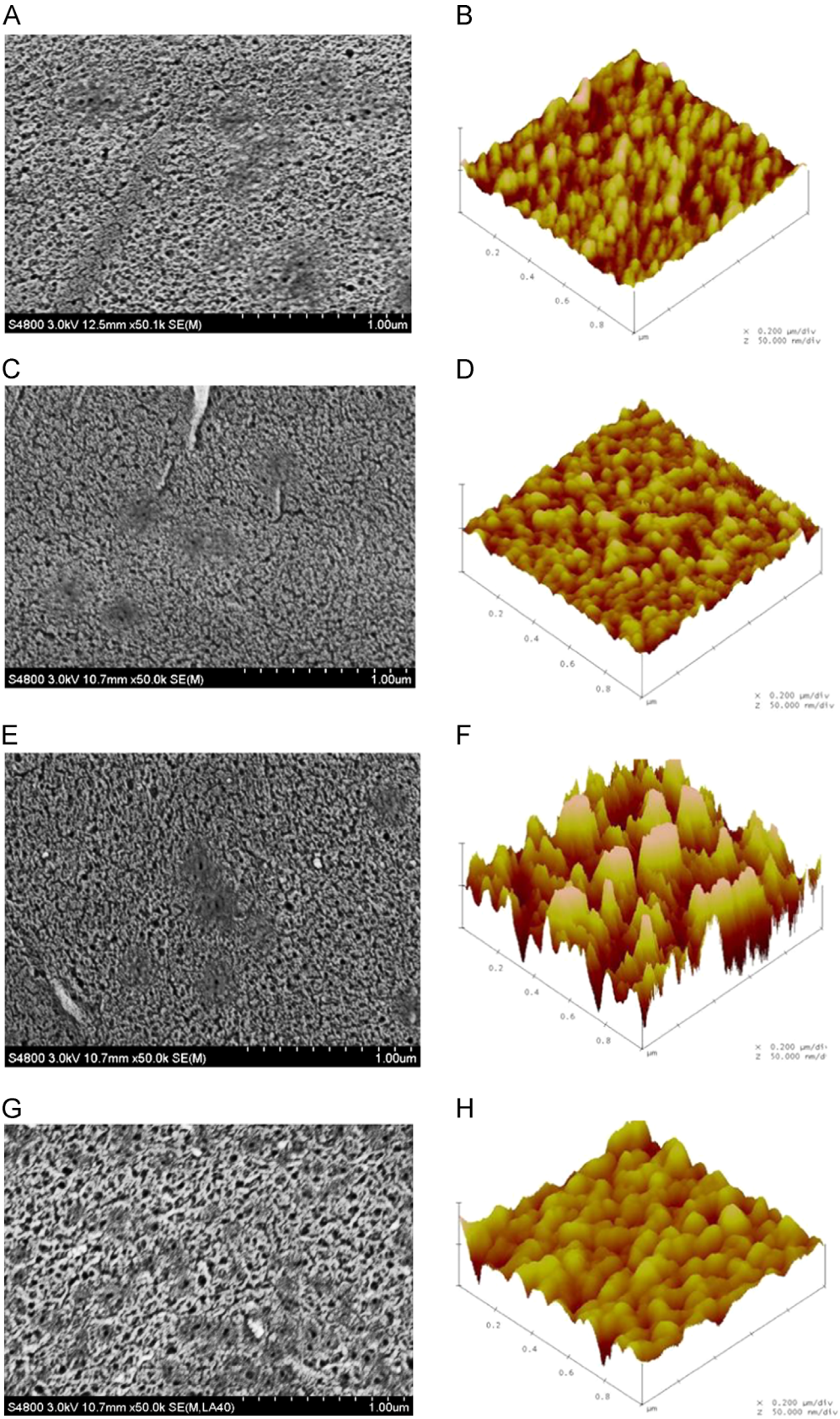


**Fig. 1.** SEM images at 50,000 × magnification and AFM images of the base PES and LbL-modified membranes. (A) and (B) Base PES; (C) and (D) 0.1-$(CHI)_1$; (E) and (F) 0.1-$(CHI)_1$-0.5Ag; (G) and (H) 0.1-$(CHI/ALG)_1$CHI-PEGylated 0.5Ag. All AFM scans were obtained using tapping mode in high purity water. Coating time was 30 min.

roughness, with the exception of membrane encoded 0.1-(CHI/ALG)$_1$CHI-PEGylated 0.5Ag, which contains PEGylated AgCl/TiO$_2$ in the outmost layer and has a relatively high roughness of ~16 nm. Cross-sectional SEM images (Supplementary data, Fig. A4) are unfortunately unable to resolve the adsorbed surface layers.

The measurement of surface roughness can provide valuable information of interest for the study of fouling on membrane surfaces. However, the interplay between surface fouling and roughness is complex, and the effects of roughness on membrane fouling can vary depending on the foulant-membrane interactions, especially the interplay between the size of foulant particulates, roughness and morphology of the fouled surface [19,20]. Conventionally, an increase in surface roughness would be expected to lead to a reduction in the contact area between a foulant particle and a planar surface with which it interacts due to the presence of asperities on the surface. Several models have been proposed using some measure of surface roughness to account for the reduced contact area between a particle and a rough surface [21–23]. Rabinovich et al. [24] calculated that a surface RMS roughness of only 1.6 nm could lead to a fivefold decrease in adhesion forces, from which a perfectly smooth surface would be expected normally. However, when examining the fouling of membrane surfaces during filtration tests, many researchers have found a strong correlation between surface roughness and fouling [25]. For instance, it has been shown that cellulose acetate (CA) membranes are less prone to fouling than the rougher polyamide membranes [26]. This was associated with a lower shear rate over the higher roughness structures as well as with less favorable acid base interactions [27]. Rana et al. [28] found a linear correlation between flux reduction due to fouling and surface roughness for unmodified and modified PES membranes. RMS roughness results in Fig. 2 show that AgCl/TiO$_2$-incorporated 1.5 bilayer membranes in general, with the exception of membrane encoded 0.1-(CHI/ALG)$_1$CHI-PEGylated 0.5Ag, display a lower surface roughness compared to that of AgCl/TiO$_2$-incorporated single layer membranes. Decreased surface roughness with increasing number of PEMs have been observed also by Ishigami et al. who used LbL assembly to modify a reverse osmosis membrane with poly (sodium 4-styrenesulfonate) and poly(allylamine hydrochloride) polyelectrolytes [29].

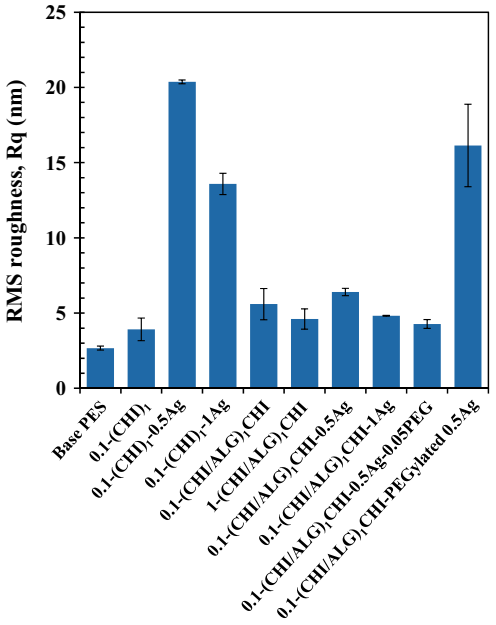


**Fig. 2.** Root mean squared roughness (RMS) of samples obtained from AFM scans of $1 \times 1\ \mu m^2$ areas. Each figure is the mean value of three measurements from different areas of the sample surface.

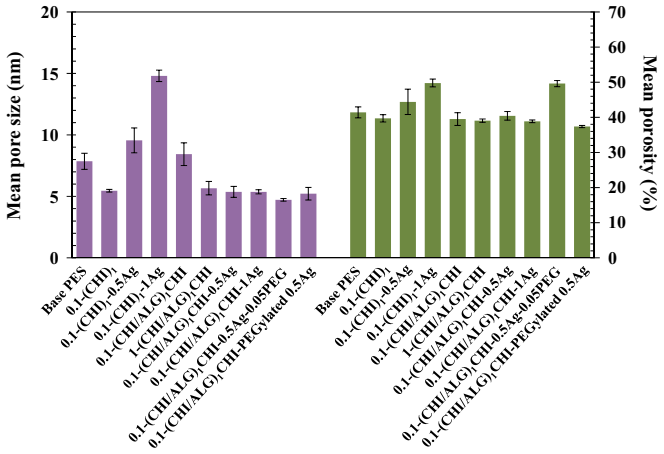


**Fig. 3.** Surface mean pore diameter shown on left, and surface mean porosity shown on right.

From the AFM data, it is possible to measure both the mean surface pore size and surface porosity. It should be emphasized that this is merely the width of the pore openings at the surface of the membrane and not the effective pore size measured by other techniques. By applying a high pass filter to the data, available in the control software, background undulations in the surface were removed. Particle analysis functions were then added with an inverted threshold to generate estimates of the mean pore diameter and pore area for each image. Multiplication of the mean pore size by the pore count for each image allowed the porosity as a percentage of the surface coverage for each scan to be calculated. The mean surface pore size is shown on the left in Fig. 3. Several of the LbL-modified samples have larger measured surface pores sizes than the unmodified membrane, suggesting that they have a more open and porous structure than the support layer. The two samples with the largest measured surface pore diameters are single layer membranes including 0.5 and 1 g/L AgCl/TiO$_2$ xerogels (encoded 0.1-(CHI)$_1$-0.5Ag and 0.1-(CHI)$_1$-1Ag) with diameters of 9.6 and 14.8 nm, respectively. Correspondingly, these two membrane preparations also have the highest measured RMS roughness. In general, it appears that we obtain smoother surfaces with reduced surface pore size with the AgCl/TiO$_2$-incorporated membranes when the PEMs are increased from single to 1.5 bilayer.

Surface porosity as determined from the mean pore area, number of pores in a scan and scan profile area are shown on right in Fig. 3 as a percentage of the surface area covered by pores. As can be seen, the calculated porosity varies between 30% and 50%, but does not show any obvious trend. It must be noted that the porosity values merely show the percentage of the surface below an arbitrary threshold (the mean height of the image in this case) and does not discriminate as to whether any channels identified as surface pores are interconnected with the void space in the membrane or not, and only shows what appear to be channels on the membrane surface. This may be the reason for why the porosity values obtained here do not show any trend or correlation with other measured parameters.

### *3.2. Effect of LbL modification on filtration and fouling of the membranes*

Most modification studies focus on a single type of fouling, yet membranes are usually subject to both organic and biological foulants concurrently during operation. We aim to combine membrane features that provide resistance to both organic and biological foulings, in addition to lasting antibacterial activity. CHI

was chosen as the outmost layer material due to its known antibacterial activity. On the other hand, cationic CHI can interact with the model foulant anionic ALG by electrostatic interaction, leading to organic fouling. For instance, Yang et al. observed that anionic human serum albumin adsorption on CHI grafted polysulfone can be as high as 30 μg/cm$^2$ [30]. In addition, Mello et al. showed 100% BSA adsorption on a CHI membrane after filtering 1 g/L BSA solution through the membrane [31]. However, in LbL-modified membranes, the surface properties are significantly affected by the interpenetration between the layers, rather than being dependent solely on the outmost layer properties. Indeed, Zhou et al. found no BSA adsorption on the surface of LbL-modified poly(lactide-co-glycolide) nanoparticles modified by coating 3 bilayer CHI/ALG PEMs with the CHI layer being the outmost [32]. This antifouling effect was associated with negative surface charge exerted by ALG chains protruding into the surface from the ALG layer assembled underneath the outmost CHI layer.

By controlling the polyelectrolyte properties and adsorption conditions, electrostatic interactions between the PEMs can be tuned to obtain the optimal surface conditions, in particular the surface charge, which is essential in imparting antifouling feature to the membrane. In this section, we present a survey of the parameters that influence the surface properties of the LbL-modified membranes to attain an optimal antifouling membrane with the outmost layer sustained as the antibacterial CHI.

### 3.2.1. *Effect of pH*

The surface composition of the membrane can be controlled by changing the PEMs assembly pH. CHI is a positively charged polymer owing to the amino groups present on the polysaccharide chain, and it has a pKa of ~6 in acidic conditions [33,34]. CHI solution is positively charged at pH values below 6 with the amount of positive charge increasing when the solution gets more acidic. The pH of the CHI solution that forms the outmost layer was changed from 5 to 6 to study the effect of less positively charged CHI surface on organic fouling, where the preceding layers were built using CHI solution at pH 5 and ALG solution at pH 7 as optimized previously. By reducing the positive charge density of the outmost CHI layer, we aimed at inducing a greater charge mismatch between the underlying negatively charged ALG layer and the outmost CHI layer. We postulate that this charge mismatch will lead to an excess of negative charge on the surface, forming a negative electrostatic barrier that extends into the solution and helps prevent deposition of foulant ALG. Table 3 lists the 1.5 bilayer LbL-modified membranes prepared with 0.1 g/L polyelectrolyte concentration when the pH of the top layer forming CHI solution is adjusted to 5 or 6, and Fig. 4 shows filtration and fouling results together with the base PES membrane.

The results indicate that although increasing the pH of the outmost CHI layer from 5 to 6 lead to a slight improvement in fouling resistance, the decrease in permeability from 665 to 281 L/m$^2$ h bar prove pH 5 to be more efficient in attaining a better overall membrane performance. The decrease in permeability is attributed to enhanced CHI deposition at pH 6 due to poorer polyelectrolyte solubility, which results in increased layer mass exerting a higher resistance to water flow. However, the CHI solution at pH 5 for forming the outmost layer results in good antifouling; the permeability decline of this membrane after ALG fouling is insignificant within the error margins.

**Table 3**
1.5 bilayer LbL-modified membranes prepared at varying pH values of the outmost layer-forming CHI solution.

| LbL layers | Polyelectr. conc. (g/L) | pH | Abbreviation |
|---|---|---|---|
| CHI/ALG/CHI | 0.1 | 5 | 0.1-(CHI/ALG)$_1$CHI-pH5 |
| CHI/ALG/CHI | 0.1 | 6 | 0.1-(CHI/ALG)$_1$CHI-pH6 |

### 3.2.2. *Effects of polyelectrolyte concentration and adsorption time*

Polyelectrolyte adsorption time is one of the parameters that impact PEM features. A low degree of adsorption of the LbL layers may result in insufficient coverage of the membrane surface, whereas a high degree modification may lead to significantly decreased permeability compared to the base membrane [35]. Therefore, polyelectrolyte adsorption time should be studied to accomplish acceptable LbL modification. The influence of adsorption time along with the polyelectrolyte concentration was investigated. Polyelectrolyte concentration was applied as 0.1 g/L or 1 g/L in forming 1.5 bilayers at adsorption times of 30 or 60 min. Table 4 lists the modified membranes studied in this section and Fig. 5 shows the water permeability of these membranes before and after ALG fouling in comparison with the base PES membrane.

Our past work showed inefficient modification at deposition times shorter than 30 min. On the other hand, any LbL modification at 30 and 60 min led to reduced permeability but enhanced antifouling performance compared to those of the base PES membrane. The permeability decline after ALG fouling was insignificant in the 30 min modified membranes. The permeability decline after ALG fouling is 53 % for the PES membrane, and 31 % and 40 % for the 1.5 bilayer membranes coated at 60 min adsorption time with 0.1 and 1 g/L polyelectrolyte solutions, respectively.

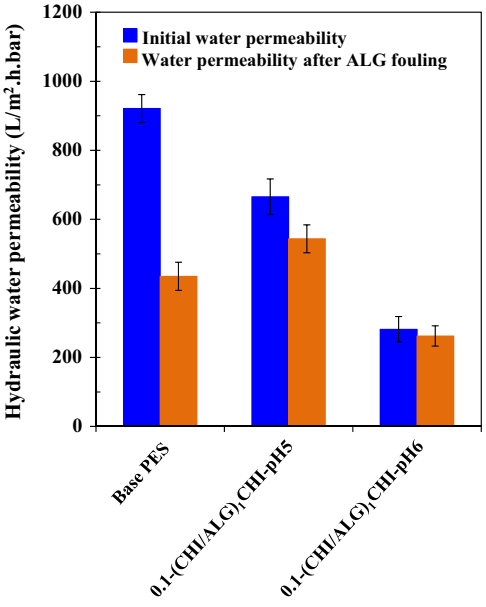


**Fig. 4.** Water permeability before and after ALG fouling of the 1.5 bilayer LbL-modified membranes prepared at varying pH values of the top layer-forming CHI solution.

**Table 4**
1.5 bilayer LbL-modified membranes prepared with varying adsorption times and polyelectrolyte concentrations.

| LbL layers | Polyelectr. conc. (g/L) | Coating time (min) | Abbreviation |
|---|---|---|---|
| CHI/ALG/CHI | 0.1 | 30 | 0.1-(CHI/ALG)$_1$CHI-30 |
| CHI/ALG/CHI | 1 | 30 | 1-(CHI/ALG)$_1$CHI-30 |
| CHI/ALG/CHI | 0.1 | 60 | 0.1-(CHI/ALG)$_1$CHI-60 |
| CHI/ALG/CHI | 1 | 60 | 1-(CHI/ALG)$_1$CHI-60 |

In fact, higher concentration PEMs were employed in an attempt to enhance the hydrophilic character of the surface. However it led to decreased surface pore opening compared to that of the low concentration PEMs (Fig. 3 left side) and poorer water permeability. In addition, extending the coating time to 60 min was found to result in a decline not only in water permeability but also in antifouling performance of the membranes. Decreased permeability at prolonged deposition time was associated with thickening of the PEMs deposited, and thus higher resistance to flow, correlated by higher mass of 60 min modified membranes at both 0.1 g/L and 1 g/L PEM concentration (Supplementary data, Fig. A5). Total amount of adsorbed PEMs did not change with increasing polyelectrolyte concentration; hence, lowering permeability at higher polyelectrolyte concentrations was attributed to smaller surface pore opening as mentioned earlier. Changes in PEM amount at the surface, presumably governed by the kinetics of ALG and CHI layer adsorption, have a major effect on changing the surface charge, explaining the antifouling performance of the membranes. Lower antifouling performance of the 60 min modified membranes imply less negatively charged surfaces that pose a weaker electrostatic barrier against ALG.

In summary, the 1.5 bilayer membrane coated at 0.1 g/L polyelectrolyte concentration for 30 min (encoded 0.1-$(CHI/ALG)_1$CHI-30) showed no organic fouling tendency and the highest water flux, ~665 L/m$^2$ h bar. This membrane has similar roughness (Fig. 2) and hydrophilicity (data not shown) compared with the commercial PES membrane. To quantify the surface charge, base PES and 0.1-$(CHI/ALG)_1$CHI-30 membranes were stained with cationic toluidine blue and anionic congo red dyes, and the intensity of each color resulting from the adsorption of dyes was measured (Supplementary data, Fig. A6). To mimic ALG fouling, the pH of the dye solution was adjusted to 7, and prior to staining, the membranes were immersed in HCl solution (used for adjusting the pH of the alginate) for 4 h to match the ALG filtration time. It was observed that color intensities measured on both the base PES and 1.5 bilayer membrane were similar when the membranes were not exposed to HCl prior to staining. On the other hand, the red dye intensity measured on HCl-treated commercial membrane increased from 12 to 22 due to adsorption of hydronium ions. In the LbL-modified membrane, HCl treatment did not change the surface charge, probably due to adsorption of hydronium ions on the inner layers rather than the outmost layer. The results show that the base PES has higher positively charged groups on the surface compared to the 1.5 bilayer membrane, allowing more ALG adsorption and thus greater permeability decline due to fouling.

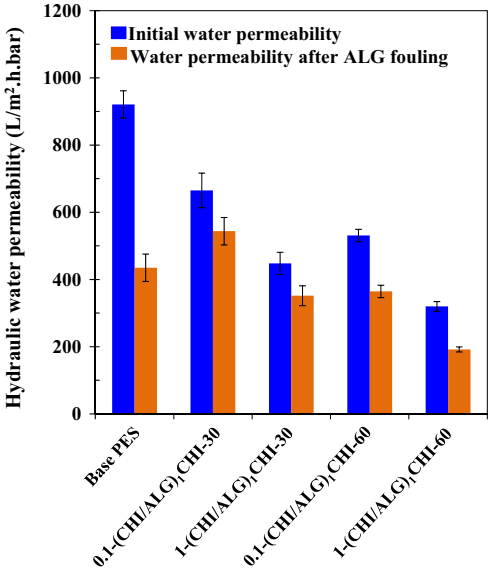


**Fig. 5.** Water permeability before and after ALG fouling of the 1.5 bilayer LbL-modified membranes prepared with varying adsorption times and polyelectrolyte concentrations.

**Table 5**
LbL-modified membranes prepared with varying number of PEMs and polyelectrolyte concentrations.

| LbL layers | Polyelectr. conc. (g/L) | Abbreviation |
|---|---|---|
| CHI/ALG/CHI | 0.1 | 0.1-$(CHI/ALG)_1$CHI |
| CHI/ALG/CHI/ALG/CHI | 0.1 | 0.1-$(CHI/ALG)_2$CHI |
| CHI/ALG/CHI/ALG/CHI/ALG/CHI | 0.1 | 0.1-$(CHI/ALG)_3$CHI |
| CHI/ALG/CHI | 1 | 1-$(CHI/ALG)_1$CHI |
| CHI/ALG/CHI/ALG/CHI | 1 | 1-$(CHI/ALG)_2$CHI |
| CHI/ALG/CHI/ALG/CHI/ALG/CHI | 1 | 1-$(CHI/ALG)_3$CHI |

### 3.2.3. *Effects of bilayer number and polyelectrolyte concentration*

It has been suggested that membrane surface roughness can be smoothed by increasing the number of LbL layers to attain better antifouling performance [35]. The number of PEMs employed as 1.5 bilayers $(CHI/ALG)_1$CHI, 2.5 bilayers $(CHI/ALG)_2$CHI and 3.5 bilayers $(CHI/ALG)_3$CHI (Table 5) and the effects of number of PEMs on water permeability and fouling resistance of the membranes are shown in Fig. 6.

Membranes modified with both 0.1 and 1 g/L polyelectrolyte concentration follow the similar trend of declining water permeability as a function of the number of PEMs, although 1 g/L PEMs display lower overall water permeability compared to that of 0.1 g/L PEMs. On the other hand, 2.5 and 3.5 bilayer membranes still show lower permeability decline, 30% in 1-$(CHI/ALG)_2$CHI and 41% in 1-$(CHI/ALG)_3$CHI, in comparison to the base PES with 53% decline. Permeability of 1.5 and 2.5 bilayer membranes at 0.1 g/L PEM concentration (encoded 0.1-$(CHI/ALG)_1$CHI and 0.1-$(CHI/ALG)_2$CHI) is very similar. These results show that 1.5 bilayer membrane modified at 0.1 g/L PEM concentration (30 min adsorption time) performs better than the other LbL-modified membranes in terms of water permeability and antifouling performance. It appears that increasing the number of PEMs exerts additional resistance to water flow.

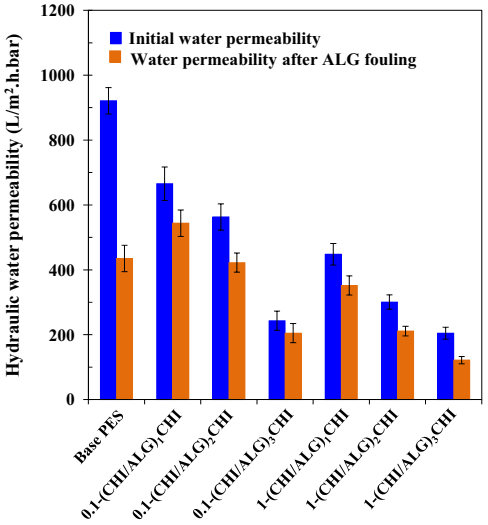


**Fig. 6.** Water permeability before and after ALG fouling of the LbL-modified membranes prepared with varying number of PEMs and polyelectrolyte concentrations.

### 3.2.4. Effect of ionic strength

By salt addition into the polyelectrolyte solution, the thickness of each individual layer can be adjusted [36–38]. To investigate the effects of increased ionic strength on PEMs, we added NaCl to the outmost layer CHI solution and modified the base membrane with different number of PEMs. Table 6 lists the LbL-modified membranes prepared with varying number of PEMs and ionic strength; the water permeability of these membranes is shown in Fig. 7 with respect to their counterparts prepared without NaCl addition.

The effect of NaCl incorporation in the coating solutions reveals itself through the decreased water permeability of NaCl-containing PEMs compared to that of those prepared without NaCl addition. The water permeability and antifouling property of NaCl-free membranes deteriorate by increasing number of PEMs, from 1.5 to 3.5. After ALG filtration, the permeability decline in 2.5 and 3.5 bilayer membranes without NaCl (encoded 1-$(CHI/ALG)_2$CHI and 1-$(CHI/ALG)_3$CHI) is 30% and 40%, respectively, while no significant drop in the water permeability of counterpart NaCl-added membranes (encoded 1-$(CHI/ALG)_2$CHI-0.1NaCl and 1-$(CHI/ALG)_3$CHI-0.1NaCl) is observed. Although the initial water permeability of 1.5 bilayer NaCl-containing membrane (encoded 1-$(CHI/ALG)_1$CHI-0.1NaCl) is higher than the other NaCl-containing membranes, its fouling resistance is not as good; its water permeability levels with the others after fouling, indicating weaker resistance to fouling.

Overall, it appears that increased ionic strength results in thicker PEMs on the membrane surface and higher resistance to water flow. This increase in layer thickness is explained by different chain conformations with and without salt in the solution: chains are aligned flat and parallel to the base surface when there is no salt, whereas when there is salt, chains form a coil conformation that later adsorb to the base surface [39,40]. Salt presence in the polyelectrolyte solution causes the screening of charges along the polyelectrolyte chains, leading to entangled polymer chains and thicker PEMs.

As a result of all improvement studies explained so far, we determined the best performing LbL membrane to be the 1.5 bilayer membrane modified with 0.1 g/L PEMs and the outmost layer CHI solution pH 5, at 30 min adsorption time. We pursued further modifications in this membrane to impart biological fouling resistance and antibacterial activity to its surface.

**Table 6**
LbL-modified membranes prepared with varying number of PEMs and ionic strength.

| LbL layers | Polyelectr. conc. (g/L) | 0.1 M NaCl addition | Abbreviation |
|---|---|---|---|
| CHI/ALG/CHI | 1 | Yes | 1-$(CHI/ALG)_1$CHI-0.1NaCl |
| CHI/ALG/CHI/ALG/CHI | 1 | Yes | 1-$(CHI/ALG)_2$CHI-0.1NaCl |
| CHI/ALG/CHI/ALG/CHI/ALG/CHI | 1 | Yes | 1-$(CHI/ALG)_3$CHI-0.1NaCl |
| CHI/ALG/CHI | 1 | No | 1-$(CHI/ALG)_1$CHI |
| CHI/ALG/CHI/ALG/CHI | 1 | No | 1-$(CHI/ALG)_2$CHI |
| CHI/ALG/CHI/ALG/CHI/ALG/CHI | 1 | No | 1-$(CHI/ALG)_3$CHI |

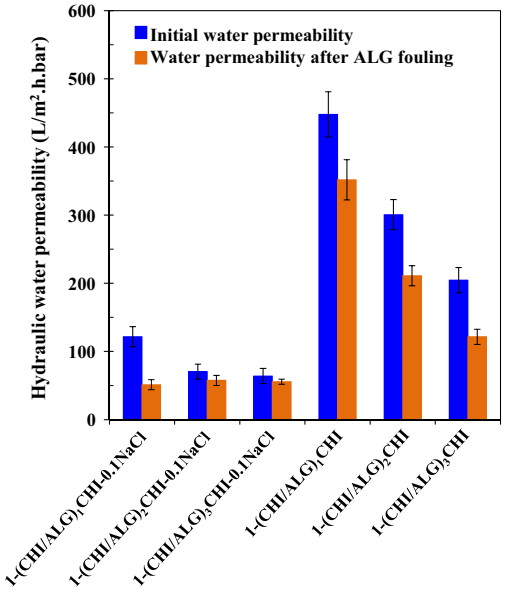


**Fig. 7.** Water permeability before and after ALG fouling of the LbL-modified membranes prepared with varying number of bilayers and ionic strength.

### 3.3. Effect of AgCl/$TiO_2$ xerogels on filtration and biofouling of the LbL modified membranes

It is known that chitosan is bactericidal whereas silver in metallic or ionic forms is highly effective in inhibiting and also killing a wide spectrum of bacteria [17,41,42]. The challenge in preparation of membranes with silver materials is twofold: 1) controlling the release rate of silver, 2) tailoring the location of silver on the membranes. We overcame these challenges by preparing AgCl/$TiO_2$ xerogels to control the release rate of silver ions and, in addition, by using the LbL method, we incorporated AgCl/$TiO_2$ xerogels only on the top layer of the membrane to enhance the anti-biofouling property. We compared the anti-biofouling properties of AgCl/$TiO_2$-incorporated membranes with the AgCl/$TiO_2$-free membranes against *E. coli* bacteria suspension in water. Anti-biofouling properties of AgCl/$TiO_2$-incorporated and AgCl/$TiO_2$-free membranes were determined by measuring the water permeability before and after *E. coli* solution filtration.

We added AgCl/$TiO_2$ xerogels in the single layer and top layer of 1.5 bilayer membranes using the procedure explained in the Section 2.3. In fact, the number of PEMs was limited to 1.5 to eliminate the permeability decline observed at increased thickness (Fig. 6). Three approaches were used to incorporate AgCl/$TiO_2$ xerogels into the single and 1.5 bilayer LbL modified membranes: 1) pure AgCl/$TiO_2$ xerogels at different concentrations; 2) PEG-mixed AgCl/$TiO_2$ xerogels; and 3) PEGylated AgCl/$TiO_2$ xerogels. Table 7 lists the membranes prepared for the biofouling study.

Fig. 8 shows that initial permeability of AgCl/$TiO_2$-free single layer membrane (encoded 0.1-$(CHI)_1$) is lower by a factor of 1.86 compared to the base membrane. On the other hand, 1.5 bilayer AgCl/$TiO_2$-free membrane (encoded 0.1-$(CHI/ALG)_1$CHI) displayed ~41% higher permeability compared to the single layer AgCl/$TiO_2$-free membrane, although one may expect lower water permeability since overall layer thickness has increased. This seems to be related to the surface hydrophilicity, however contact angle measurement of the surfaces did not show such correlation (data not shown). The lower permeability of the AgCl/$TiO_2$-free single layer membrane compared to the base PES is associated with the decrease in surface pore diameter, from ~8 nm to ~5 nm (Fig. 3, left side). The surface pore diameter of the base PES and 1.5 bilayer AgCl/$TiO_2$-free membrane is essentially the same, ~8 nm, although the water permeability of the 1.5 bilayer AgCl/$TiO_2$-free membrane is 26% lower. This again is related with resistance to water flow due to PEMs (Fig. 6). In addition, we observed that the water permeability of all AgCl/$TiO_2$-incorporated single layer membranes improved by ~29% compared to the base PES membrane, regardless of AgCl/$TiO_2$ amount loaded. On the other hand,

**Table 7**
Single layer and 1.5 bilayer LbL-modified membranes prepared by incorporating $AgCl/TiO_2$ xerogels in the outmost layer-forming CHI solution.

| LbL layers | Polyelectr. conc. (g/L) | Modification agent | Abbreviation |
|---|---|---|---|
| CHI | 0.1 | - | $0.1\text{-}(CHI)_1$ |
| CHI | 0.1 | 0.5 g/L $AgCl/TiO_2$ | $0.1\text{-}(CHI)_1$-0.5Ag |
| CHI | 0.1 | 1 g/L $AgCl/TiO_2$ | $0.1\text{-}(CHI)_1$-1Ag |
| CHI | 0.1 | 5 g/L $AgCl/TiO_2$ | $0.1\text{-}(CHI)_1$-5Ag |
| CHI/ALG/CHI | 0.1 | - | $0.1\text{-}(CHI/ALG)_1CHI$ |
| CHI/ALG/CHI | 0.1 | 0.5 g/L $AgCl/TiO_2$ | $0.1\text{-}(CHI/ALG)_1CHI$-0.5Ag |
| CHI/ALG/CHI | 0.1 | 1 g/L $AgCl/TiO_2$ | $0.1\text{-}(CHI/ALG)_1CHI$-1Ag |
| CHI/ALG/CHI | 0.1 | 2.5 g/L $AgCl/TiO_2$ | $0.1\text{-}(CHI/ALG)_1CHI$-2.5Ag |
| CHI/ALG/CHI | 0.1 | 0.5 g/L $AgCl/TiO_2$+0.05 g/L PEG | $0.1\text{-}(CHI/ALG)_1CHI$-0.5Ag-0.05PEG |
| CHI/ALG/CHI | 0.1 | 0.5 g/L PEGylated $AgCl/TiO_2$ | $0.1\text{-}(CHI/ALG)_1CHI$-PEGylated 0.5Ag |

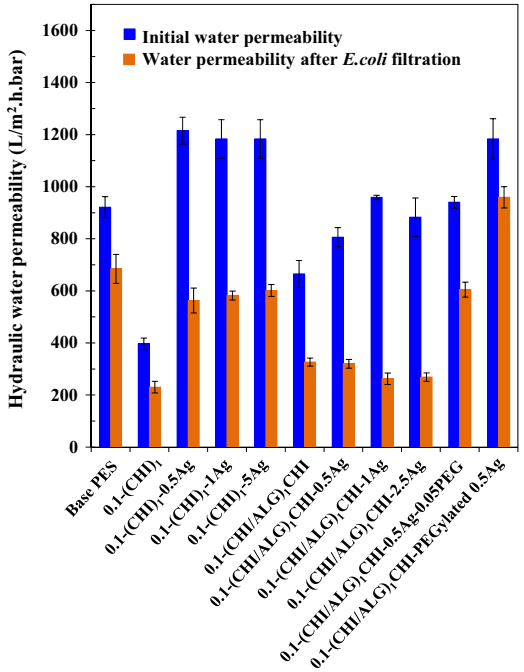


**Fig. 8.** Water permeability before and after *E. coli* bacteria adhesion on surface of the single layer and 1.5 bilayer LbL-modified membranes prepared by incorporating $AgCl/TiO_2$ xerogels in the top layer-forming CHI solution.

the water permeability of all $AgCl/TiO_2$-incorporated 1.5 bilayer membranes was the same as that of the base PES within our experimental uncertainties. The increase in water permeability observed on all $AgCl/TiO_2$-incorporated single layer membranes is correlated with the increase in surface roughness (Fig. 2) and surface pore diameter (Fig. 3 left side) compared to the base PES.

In $AgCl/TiO_2$-incorporated layer preparation, PEG has been used as a stabilizing agent and dispersant for $AgCl/TiO_2$ xerogels in CHI solution. PEG treatment of $AgCl/TiO_2$ xerogels has been conducted with two methods: (1) PEGylation of $AgCl/TiO_2$ xerogels before adding into the outmost layer CHI solution (membrane encoded $0.1\text{-}(CHI/ALG)_1$CHI-PEGylated 0.5Ag), and (2) simultaneous addition of $AgCl/TiO_2$ xerogels and PEG into the outmost layer CHI solution (membrane encoded $0.1\text{-}(CHI/ALG)_1$CHI-0.5Ag-0.05 PEG). PEGylation resulted in ~25% improvement in initial water permeability and much better biological fouling resistance compared with the other treatment. The better performance was associated with the high surface roughness of PEGlayted $AgCl/TiO_2$-incorporated 1.5 bilayer membrane, which is ~12 nm, where the PEG-mixed $AgCl/TiO_2$-incorporated 1.5 bilayer membrane and the base PES both have a surface roughness of ~2.5 nm (Fig. 2). In fact, our observation on the high water permeability with rougher surfaces parallels the findings of Hashino et al. [43]. Except for membranes with PEG-treated PEMs, biological fouling led to a ~50% permeability decline in all other membranes. Permeability decline was 20% for the PEGlayted $AgCl/TiO_2$-incorporated membrane, 26% for the PEG-mixed $AgCl/TiO_2$-modified membrane, and 34% for the base PES membrane.

The surface element mapping of the membranes prepared with $AgCl/TiO_2$ xerogels showed that pure $AgCl/TiO_2$ and PEGlayted $AgCl/TiO_2$ addition results in uniform distribution of the Ag, Cl, Ti and O elements while non-uniform element distribution occurs on the surface of PEG-mixed $AgCl/TiO_2$-incorporated membrane (Supplementary data, Figs. A7–A9). We quantitatively found, from the EDX analyses conducted on different parts of the surface, that weight percentage of Ag and Ti on the surface of PEGlayted $AgCl/TiO_2$ membrane is twice that of found on the other two membranes. This indicates surface enrichment in Ag and Ti elements when $AgCl/TiO_2$ xerogels are in PEGylated form. This finding agrees well with the studies which show that coordination of PEG to metal–metal complexes in solution leads to surface enrichment of some elements, e.g. manganese enrichment in the iron-manganese alloy materials [44–46].

### 3.4. Stability of LbL-modified layers

#### 3.4.1. Stability of the $AgCl/TiO_2$-free polyelectrolyte layers

CHI and ALG PEMs in contact with high concentration NaCl may experience conformation change due to the screening effect of $Na^+$ and $Cl^-$ ions, leading to decomplexation and removal of the adsorbed CHI and ALG layers [8]. Stability of PEMs prepared without $AgCl/TiO_2$ addition has been studied by testing the water permeability of the membranes immediately after LbL modification, following 7-day storage in 1 M NaCl solution and 14-day storage in 1 M NaCl solution. 1.5 bilayer membranes modified at 0.1 g/L polyelectrolyte concentration for 30 min, were used in the stability tests. We found that water permeability stayed constant at ~650 $L/m^2$ h bar within the uncertainty of our measurements in all stability test conditions (data is not shown). In the case of weakly adsorbed PEMs, one could expect an increase in water permeability due to the removal of layers from the surface. We determined that the PEMs in this study were strong and stable because there was no observed change in water permeability, even after 14-days storage in 1 M NaCl solution.

#### 3.4.2. Stability of the $AgCl/TiO_2$-incorporated polyelectrolyte layers

It is well known that silver nanoparticles are soluble in water [47,48]. For instance, Tuncer and Seker [17] reported very high dissolution for silver nanoparticles from $Ag/TiO_2$ xerogels produced with the same sol–gel method used in this study. In contrast, they found very low dissolution for AgCl in water due to fast reaction between $Ag^+$ and $Cl^-$ ions in water. This reaction

indicated below leads to precipitation of AgCl where the reverse reaction is very slow with an equilibrium solubility constant of $\sim 1.12 \times 10^{-10}$ mol$^2$/L$^2$ at 18 °C for AgCl in water [49].

$$Ag^{+}_{(aq)} + Cl^{-}_{(aq)} \leftarrow \rightarrow AgCl_{(aq)}$$

Therefore, we found it promising to synthesize AgCl particles in $TiO_2$ to control the release rate of silver, targeting long term durability for the AgCl/$TiO_2$-incorporated membranes. To prove our hypothesis on controlled silver release, silver leach from the AgCl/$TiO_2$-incorporated PEMs to the permeate side of the dead-end cell filtration system was monitored during deionized water filtration using ICP-MS.

The PEGylated AgCl/$TiO_2$-incorporated membrane (encoded 0.1-(CHI/ALG)$_1$CHI-PEGylated 0.5Ag), which showed the highest permeability among all membranes ($\sim$1000 L/m$^2$ h), was used in the silver release tests. Silver amount in consecutively collected permeate samples was quantified. Silver concentration (μg/L) and the cumulative silver amount (μg/m$^2$) are shown as a function of filtration (L/m$^2$) in Fig. 9. We found that silver loss per filtration stayed constant at $\sim$7.44 μg/L after a filtration totaling 3000 L/m$^2$. To the best of our knowledge, this is the first study reporting a low silver release at a constant rate from LbL modified membranes for a high filtration volume obtained at a high filtration rate. For instance, Zodrow et al. [10] reported no silver detection in the filtrate of a dead-end filtration module after approximately 3100 L/m$^2$ filtration through a silver nanoparticle loaded polysulfone membrane (nAg-PSf). On the other hand, it should be noted that water permeability of nAg-PSf membrane ($\sim$144 L/m$^2$ h) used by Zodrow et al. [10] is 6.9 times lower than the permeability of LbL-modified membrane used in this study (0.1-(CHI/ALG)$_1$CHI-PEGylated 0.5Ag). We propose that silver release rate can be controlled even at a significantly high filtration rate by using AgCl/$TiO_2$ xerogels with the added advantage of immobilization solely on the membrane surface by LbL assembly.

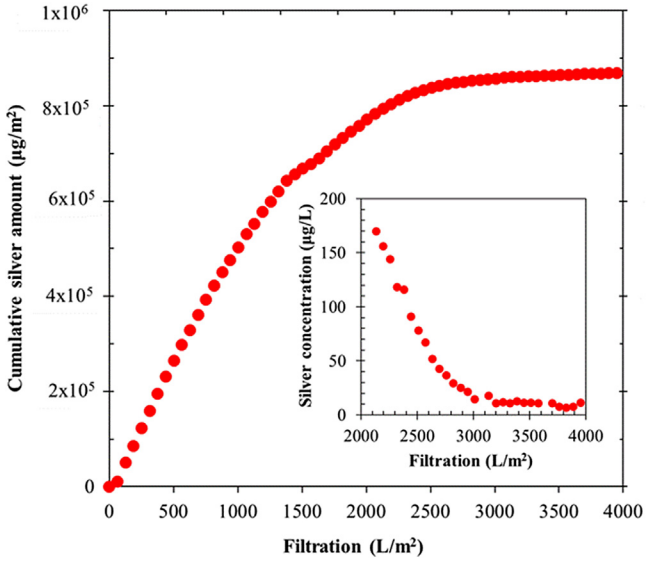


**Fig. 9.** Cumulative silver amount release, μg/m$^2$, with dead-end filtration of deionized water from 0.1-(CHI/ALG)$_1$CHI-PEGylated 0.5Ag membrane (Inset: silver concentration, μg/L, in the filtrate as a function of filtration, L/m$^2$).

From Fig. 9, one could calculate how long it will take the silver to be released completely from 0.1-(CHI/ALG)$_1$CHI-PEGylated 0.5Ag membrane at the filtration rate $\sim$1000 L/m$^2$ h. Up to a filtration volume totaling 3000 L/m$^2$, silver loss per filtration cycle increased, leading to 4.2% reduction in the immobilized silver amount. After that, silver loss per filtration cycle stabilized at $\sim$7.44 μg/L, which extrapolates to $\sim$265 days for the remaining silver to be lost. Although this release time span may appear relatively short in terms of practical applications, we suggest that loading higher amount of AgCl/$TiO_2$ in the LbL layer and employing slower filtration rates could easily extend the silver consumption time. Nonetheless, we have proven that silver release could be governed by use of AgCl/$TiO_2$ xerogels rather than silver nanoparticles and LbL technique enables us to immobilize the silver specifically in the outmost layer.

### 3.5. Antibacterial properties of the membranes

The antibacterial activity of the base PES and LbL-modified membranes was measured against *E. coli*. To differentiate between the bactericidal properties of the positively charged chitosan and AgCl/$TiO_2$ particles, we performed antibacterial activity measurements on three membranes simultaneously: (1) base PES membrane, (2) 1.5 bilayer membrane modified at 0.1 g/L polyelectrolyte concentration (0.1-(CHI/ALG)$_1$CHI), (3) pure AgCl/$TiO_2$-incorporated membrane (0.1-(CHI/ALG)$_1$CHI-0.5Ag), (4) PEG-mixed AgCl/$TiO_2$-incorporated membrane (0.1-(CHI/ALG)$_1$CHI-0.5Ag-0.05PEG), and (5) PEGylated AgCl/$TiO_2$-incorporated membrane (0.1-(CHI/ALG)$_1$-CHI-PEGylated 0.5Ag). Antibacterial activities of all membranes were determined using an aerobic plate count on the membrane surface. Fig. 10 shows the light microscope photos of the base PES and selected LbL-modified membranes, taken after overnight incubation with *E. coli* bacteria on Mueller-Hinton agar plates at 37 °C.

All membranes modified with AgCl/$TiO_2$ xerogels display a cell count of zero on the surface, where the average number of CFU counted on the surface of AgCl/$TiO_2$-free 1.5 bilayer membranes

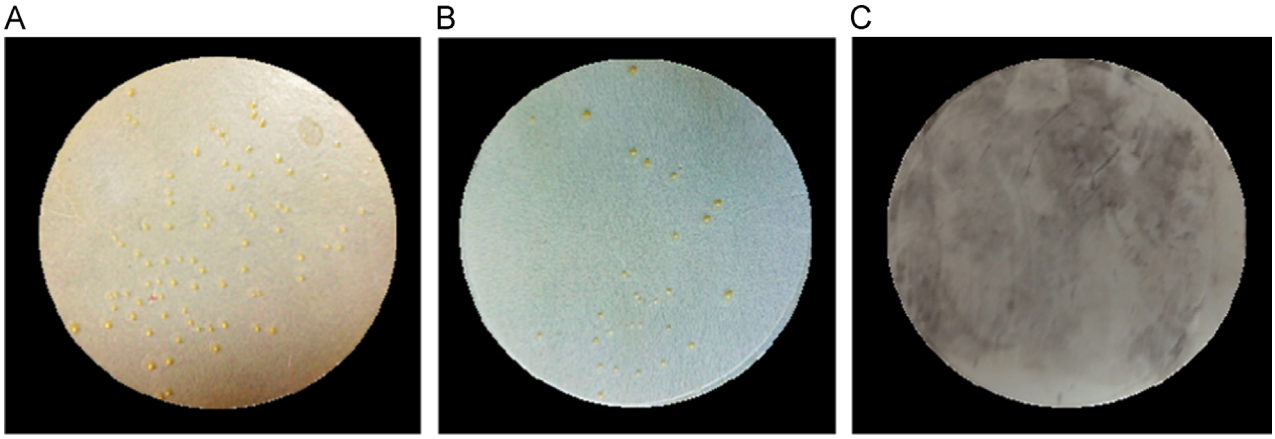


**Fig. 10.** Antibacterial effect on *E. coli*. (A) Base PES membrane; (B) 1.5 bilayer membrane modified at 0.1 g/L polyelectrolyte concentration ([0.1-(CHI/ALG)$_1$CHI]); (C) PEGylated AgCl/$TiO_2$-incorporated membrane ([0.1-(CHI/ALG)$_1$CHI-PEGylated 0.5Ag]).

was 54. This result shows that the outmost CHI layer could hinder bacterial growth to some extent, provided that the number of CFU seeded initially was 60. On the other hand, the base PES membrane experienced extensive bacterial growth; 77 CFU on average were counted on the membrane surface. These results agree with the work of Qi et al. [50] who proposed that positively charged CHI particles in contact with negatively charged cell membranes lead to increased cell membrane permeability, leading to rupture and leakage of intracellular components of the bacteria. Similarly, Rabea et al. [51] postulated that composite membranes with a 50 nm thick chitosan layer deposited on a poly(acrylic acid)/poly (ethylene glycol) diacrylate layer possess antibacterial activity towards Gram-positive and Gram-negative bacteria and, in addition, the antibacterial activity improves with increasing CHI content.

Antibacterial activity results clearly indicate that although the CHI polycation layer provides some antibacterial property to the PES membrane, the presence of AgCl/$TiO_2$ xerogels on the surface not only hinders bacterial growth but also kills bacteria. Our silver release results indicate that AgCl/$TiO_2$- incorporated membranes have long-term antibacterial/anti-biofouling performance because there is always some small amount of silver released, i.e. $\sim$7.44 μg/L. It is well-known that a small amount of silver will suffice to inhibit bacterial growth [17]. Our conclusion is also in agreement with the study of Tuncer and Seker [17], which reports that the AgCl/$TiO_2$ xerogel powder could be used several times for more than six days without losing its antibacterial activity.

## 4. Conclusion

We have demonstrated that the LbL assembly method using CHI/ALG polyelectrolytes in combination with the AgCl/$TiO_2$ xerogels could easily be employed to impart high water permeability, low organic fouling, low biological fouling, and long-lasting antibacterial activity to the commercial PES membrane.

The water permeability of all 1.5 bilayer AgCl/$TiO_2$-incorporated membranes was found to be the same as base PES membrane. In addition, presence of AgCl/$TiO_2$ xerogels in the outmost LbL layer granted biological fouling resistance and antibacterial activity to the membrane. Best results were obtained with PEGylated AgCl/$TiO_2$ xerogels because this treatment of AgCl/$TiO_2$ led to a more uniform dispersion of silver on the membrane surface, apprized by improved water permeability and biological fouling resistance. Silver release tests indicated a 265-day lifespan for the PEGylated AgCl/$TiO_2$-incorporated membranes.

For future work, we would like to suggest a study that further explores the possibility of lowering silver release (even though the silver loss was found low in this study) by changing the texture of AgCl/$TiO_2$ xerogels, such as the pore size of $TiO_2$ and the crystallite size of AgCl. In addition, AgCl/$TiO_2$-incorporated membrane could be combined with UV and visible light source to enhance the antibacterial/biological fouling resistance performance for potential use in photocatalytic MBR systems since $TiO_2$ is a well-known photocatalyst.

## Acknowledgment

The research leading to these results has received funding from the European Union's Seventh Framework Programme (FP7/2007-2013) under grant agreement no 246039. We acknowledge Dane Rusçuklu and Canbike Bar for assistance with the filtration experiments, Evrim Paşık for assistance with the antibacterial tests, Selcan Ateş and Emre Demirkaya for the synthesis of AgCl/$TiO_2$ particles and Sanem Ezgi Kınal for ICP-MS analysis. We are also indebted to the Biotechnology and Bioengineering Application Research Center, and Environmental Research Center at the Izmir Institute of Technology for their kind help and technical support.

## Appendix A. Supporting information

Supplementary data associated with this article can be found in the online version at http://dx.doi.org/10.1016/j.memsci.2015.05.048.

## References

[1] S.F. Boerlage, M.D. Kennedy, P.A. Bonne, G. Galjaard, J.C. Schippers, Prediction of flux decline in membrane systems due to particulate fouling, Desalination 113 (1997) 231–233.
[2] Y. Kouwonou, R. Malaisamy, K.L. Jones, Modification of PES membrane: reduction of biofouling and improved flux recovery, Sep. Sci. Technol. 43 (2008) 4099–4112.
[3] C. Ba, J. Economy, Preparation and characterization of a neutrally charged antifouling nanofiltration membrane by coating a layer of sulfonated poly (ether ether ketone) on a positively charged nanofiltration membrane, J. Membr. Sci. 362 (2010) 192–201.
[4] C. Ba, D.A. Ladner, J. Economy, Using polyelectrolyte coatings to improve fouling resistance of a positively charged nanofiltration membrane, J. Membr. Sci. 347 (2010) 250–259.
[5] N. Hilal, O.O. Ogunbiyi, N.J. Miles, R. Nigmatullin, Methods employed for control of fouling in MF and UF membranes: a comprehensive review, Sep. Sci. Technol. 40 (2005) 1957–2005.
[6] C. Ba, J. Langer, J. Economy, Chemical modification of P84 copolyimide membranes by polyethylenimine for nanofiltration, J. Membr. Sci. 327 (2009) 49–58.
[7] J. Wang, Y. Yao, Z. Yue, J. Economy, Preparation of polyelectrolyte multilayer films consisting of sulfonated poly (ether ether ketone) alternating with selected anionic layers, J. Membr. Sci. 337 (2009) 200–207.
[8] R.H. Lajimi, E. Ferjani, M.S. Roudesli, A. Deratani, Effect of LbL surface modification on characteristics and performances of cellulose acetate nanofiltration membranes, Desalination 266 (2011) 78–86.
[9] S.T. Kang, A. Subramani, E. Hoek, M.A. Deshusses, M.R. Matsumoto, Direct observation of biofouling in cross-flow microfiltration: mechanisms of deposition and release, J. Membr. Sci. 244 (2004) 151–165.
[10] K. Zodrow, L. Brunet, S. Mahendra, D. Li, A. Zhang, Q. Li, P.J. Alvarez, Polysulfone ultrafiltration membranes impregnated with silver nanoparticles show improved biofouling resistance and virus removal, Water Res. 43 (2009) 715–723.
[11] T.A. Dankovich, D.G. Gray, Bactericidal paper impregnated with silver nanoparticles for point-of-use water treatment, Environ. Sci. Technol. 45 (2011) 1992–1998.
[12] R. Malaisamy, D. Berry, D. Holder, L. Raskin, L. Lepak, K.L. Jones, Development of reactive thin film polymer brush membranes to prevent biofouling, J. Membr. Sci. 350 (2010) 361–370.
[13] M.S. Mauter, Y. Wang, K.C. Okemgbo, C.O. Osuji, E.P. Giannelis, M. Elimelech, Antifouling ultrafiltration membranes via post-fabrication grafting of biocidal nanomaterials, ACS Appl. Mater. Interfaces 3 (2011) 2861–2868.
[14] F. Diagne, R. Malaisamy, V. Boddie, R.D. Holbrook, B. Eribo, K.L. Jones, Polyelectrolyte and silver nanoparticle modification of microfiltration membranes to mitigate organic and bacterial fouling, Environ. Sci. Technol. 46 (2012) 4025–4033.
[15] S. Loher, O.D. Schneider, T. Maienfisch, S. Bokorny, W.J. Stark, Micro-organism-triggered release of silver nanoparticles from biodegradable oxide carriers allows preparation of self-sterilizing polymer surfaces, Small 4 (2008) 824–832.
[16] K.P. Dobmeier, Xerogel Coatings for Biomedical Sensing Applications Order no. 3289125, The University of North Carolina at Chapel Hill ProQuest Information and Learning Company, Ann Arbor, MI, 2007.
[17] M. Tuncer, E. Seker, Single step sol–gel made silver chloride on Titania xerogels to inhibit E. coli bacteria growth: effect of preparation and chloride ion on bactericidal activity, J. Sol–Gel Sci. Technol. 59 (2011) 304–310.
[18] A. Tiraferri, M. Elimelech, Direct quantification of negatively charged functional groups on membrane surfaces, J. Membr. Sci. 389 (2012) 499–508.
[19] R.W. Bowen, T.A. Doneva, Atomic force microscopy studies of membranes: effect of surface roughness on double-layer interactions and particle adhesion, J. Colloid Interface Sci. 229 (2000) 544–549.
[20] E. Guillen-Burrieza, R. Thomas, B. Mansoor, D. Johnson, N. Hilal, H. Arafat, Effect of dry-out on the fouling of PVDF and PTFE membranes under conditions simulating intermittent seawater membrane distillation (SWMD), J. Membr. Sci. 438 (2013) 126–139.
[21] K. Cooper, N. Ohler, A. Gupta, S. Beaudoin, Analysis of contact interactions between a rough deformable colloid and a smooth substrate, J. Colloid Interface Sci. 222 (2000) 63–74.
[22] K. Cooper, A. Gupta, S. Beaudoin, Simulation of the adhesion of particles to surfaces, J. Colloid Interface Sci. 234 (2001) 284–292.

[23] C.S. Hodges, L. Looi, J.A. Cleaver, M. Ghadiri, Use of the JKR model for calculating adhesion between rough surfaces, Langmuir 20 (2004) 9571–9576.
[24] Y.L. Rabinovich, J.J. Adler, A. Ata, R.K. Singh, B.M. Moudgil, Adhesion between nanoscale rough surfaces: II. Measurement and comparison with theory, J. Colloid Interface Sci. 232 (2000) 17–24.
[25] V. Kochkodan, D.J. Johnson, N. Hilal, Polymeric membranes: surface modification for minimizing (bio)colloidal fouling, Adv. Colloid Interface Sci. 206 (2014) 116–140.
[26] M. Elimelech, X.H. Zhu, A.E. Childress, S.K. Hong, Role of membrane surface morphology in colloidal fouling of cellulose acetate and composite aromatic polyamide reverse osmosis membranes, J. Membr. Sci. 127 (1997) 101–109.
[27] E.M. Vrijenhoek, S. Hong, M. Elimelech, Influence of membrane surface properties on initial rate of colloidal fouling of reverse osmosis and nanofiltration membranes, J. Membr. Sci. 188 (2001) 115–128.
[28] D. Rana, T. Matsuura, R.M. Narbaitz, K.C. Khulbe, Influence of hydroxyl-terminated polybutadiene additives on the poly(ether sulfone) ultrafiltration membranes, J. Appl. Polym. Sci. 101 (2006) 2292–2303.
[29] T. Ishigami, K. Amano, A. Fujii, Y. Ohmukai, E. Kamio, T. Maruyama, H. Matsuyama, Fouling reduction of reverse osmosis membrane by surface modification via layer-by-layer assembly, Sep. Purif. Technol. 99 (2012) 1–7.
[30] M.C. Yang, W.C. Lin, Protein adsorption and platelet adhesion of polysulfone membrane immobilized with chitosan and heparin conjugate, Polym. Adv. Technol. 14 (2003) 103–113.
[31] R.S. Mello, G.C. Bedendo, F. Nome, H.D. Fiedler, M.C. Laranjeira, Preparation of chitosan membranes for filtration and concentration of compounds under high pressure process, Polym. Bull. 56 (2006) 447–454.
[32] J. Zhou, G. Romero, E. Rojas, L. Ma, S. Moya, C. Gao, Layer by layer chitosan/alginate coatings on poly (lactide-co-glycolide) nanoparticles for antifouling protection and Folic acid binding to achieve selective cell targeting, J. Colloid Interface Sci. 345 (2010) 241–247.
[33] A. Denuziere, D. Ferrier, A. Domard, Chitosan-chondroitin sulfate and chitosan-hyaluronate polyelectrolyte complexes. Physico-chemical aspects, Carbohydr. Polym. 29 (1996) 317–323.
[34] M. Rinaudo, M. Milas, P. Le Dung, Characterization of chitosan. Influence of ionic strength and degree of acetylation on chain expansion, Int. J. Biol. Macromol. 15 (1993) 281–285.
[35] V. Kochkodan, N. Hilal, A comprehensive review on surface modified polymer membranes for biofouling mitigation, Desalination 356 (2015) 187–207.
[36] Y. Lvov, G. Decher, H. Moehwald, Assembly, structural characterization, and thermal behavior of layer-by-layer deposited ultrathin films of poly (vinyl sulfate) and poly (allylamine), Langmuir 9 (1993) 481–486.
[37] G. Decher, J. Schmitt, Fine-tuning of the film thickness of ultrathin multilayer films composed of consecutively alternating layers of anionic and cationic polyelectrolytes, Prog. Colloid Polym. Sci. 89 (1992) 160–164.
[38] J. de Grooth, R. Oborný, J. Potreck, K. Nijmeijer, W.M. de Vos, The role of ionic strength and odd–even effects on the properties of polyelectrolyte multilayer nanofiltration membranes, J. Membr. Sci. 475 (2015) 311–319.
[39] H.A. Van der Schee, J. Lyklema, A lattice theory of polyelectrolyte adsorption, J. Phys. Chem. 88 (1984) 6661–6667.
[40] M.R. Bohmer, O.A. Evers, J.M. Scheutjens, Weak polyelectrolytes between two surfaces: adsorption and stabilization, Macromolecules 23 (1990) 2288–2301.
[41] M. Kawashita, S. Toda, H.M. Kim, T. Kokubo, N. Masuda, Preparation of antibacterial silver-doped silica glass microspheres, J. Biomed. Mater. Res. A 66 (2003) 266–274.
[42] A. Gupta, M. Maynes, S. Silver, Effects of halides on plasmid-mediated silver resistance in Escherichia coli, Appl. Environ. Microbol. 64 (1998) 5042–5045.
[43] M. Hashino, T. Katagiri, N. Kubota, Y. Ohmukai, T. Maruyama, H. Matsuyama, Effect of surface roughness of hollow fiber membranes with gear-shaped structure on membrane fouling by sodium alginate, J. Membr. Sci. 366 (2011) 389–397.
[44] R.D. Rogers, M.L. Jezl, C.B. Bauer, Effect of polyethylene glycol on the coordination sphere of strontium in $SrCl_2$ and $Sr(NO_3)_2$ complexes, Inorg. Chem. 33 (1994) 5682–5692.
[45] J.C. Yang, Y.G. Shul, Effects of ethylene glycol addition on the properties of Ru/$Al_2O_3$ catalyst prepared by sol–gel method, Catal. Lett. 36 (1996) 41–49.
[46] S. Suzuki, T. Yamamoto, H. Fukai, K. Shinoda, Enrichment and depletion of alloying elements in surface layers of iron base alloys annealed under different conditions, Int. J. Mater. Res. 100 (2009) 1255–1259.
[47] O. Akhavan, E. Ghaderi, Bactericidal effects of Ag nanoparticles immobilized on surface of $SiO_2$ thin film with high concentration, Curr. Appl. Phys. 9 (2009) 1381–1385.
[48] A. Balamurugan, G. Balossier, D. Laurent-Maquin, S. Pina, A.H.S. Rebelo, J. Faure, J.M.F. Ferreira, An in vitro biological and anti-bacterial study on a sol–gel derived silver-incorporated bioglass system, Dent. Mater. 24 (2008) 1343–1351.
[49] Knovel Critical Tables (2008), 2nd ed., Knovel Corporation, Online version available at: ⟨http://app.knovel.com/hotlink/toc/id:kpKCTE000X/knovel-critical-tables⟩.
[50] L. Qi, Z. Xu, X. Jiang, C. Hu, X. Zou, Preparation and antibacterial activity of chitosan nanoparticles, Carbohydr. Res. 339 (2004) 2693–2700.
[51] E.I. Rabea, M.E.T. Badawy, C.V. Stevens, G. Smagghe, W. Steurbaut, Chitosan as antimicrobial agent: applications and mode of action, Biomacromolecules 4 (2003) 1457–1465.